Strong Coupling Assisted by High-Q mode in Perovskite Nanodisk

Yuan Zhang
School of Electronic and Computer Engineering
Peking University
Shenzhen, China
2101212733@stu.pku.edu.cn

Jiayao Huang
School of Electronic and Computer Engineering
Peking University
Shenzhen, China
huangjiayao@pku.edu.cn

Feng Ye
School of Electronic and Computer Engineering
Peking University
Shenzhen, China
ye-feng@pku.edu.cn

H. Y. Fu
Tsinghua Shenzhen International Graduate School
Tsinghua University
Shenzhen, China
hyfu@sz.tsinghua.edu.cn

Qian Li*
School of Electronic and Computer Engineering
Peking University
Shenzhen, China
liqian@pkusz.edu.cn

***Abstract*—We design the perovskite nanodisk supporting the strong coupling between quasi-bound state in the continuum and exciton. The two-coupled oscillators model is employed to quantitatively explore the strong coupling with Rabi splitting of 300.7 meV.**

Keywords—Bound state in the continuum, Perovskite Nanodisk, Strong coupling

I. INTRODUCTION

Bound state in the continuum (BIC) corresponds to the non-radiating resonance with infinite quality factor (Q factor) which coexists within the extended-spectrum without leak of energy [1]. The concept of BIC was originally proposed in the electronic system by von Neumann and Wigner within the context of Schrödinger equation [2]. Owing to common properties related to the wave, this exotic state can be generalized from quantum physics to other fields, such as acoustic, water waves and electromagnetic. Recently, BIC based on photonic structures has arisen as a striking focus. Hence, different types of BIC were thoroughly investigated and demonstrated, such as symmetry-protected BIC and Friedrich-Wintgen BIC. In 2011, by introducing a refractive index gradient, symmetry-protected BIC was experimentally realized in a coupled-waveguide array, which provided inspiration to manipulate optical traps for small particles [3]. The instances of Friedrich-Wintgen BIC have also emerged as a dark state in the coupled photonic crystal slabs where a huge enhancement of the optical forces was obtained [4]. Besides, after being transformed into a leaky mode, BIC will collapse into quasi-BIC (QBIC) with ultra-high Q factor, which is usually accompanied by extreme field enhancement inside the structure. This prominent feature makes QBIC become a promising way to boost light-matter interaction.

In recent years, halide perovskites have emerged as an excellent platform used for enhancing light-matter interaction due to the exceptional merits including high refractive index, low intrinsic loss, simplicity of fabrication and easiness of engineering [5]. Besides, the excitons of perovskite possess high binding energy and strong oscillator strength, which allows perovskite to serve as an ideal platform to explore strong coupling. In 2022, a perovskite metasurface was proposed to realize the magnetic quadrupole-exciton strong coupling with Rabi splitting of 230.7 meV [6]. This work shows that the strong coupling between light and exciton leads to the generation of exciton-polaritons which are half-light, half-matter quasiparticles. Exciton-polaritons exhibit the advantages of rapid propagation, strong coherence and low effective mass [7]. Such properties allow exciton-polaritons to be a brightening platform for basic physics research including Bose-Einstein Condensation [8], and also offer a feasible strategy for designing polariton nano-lasers [9] and realizing all-optical switches and transistors [10], [11]. It is highly desirable to seek original designs which incorporate the QBIC into the perovskite material in the strong coupling regime. Because of the high Q factor and giant field enhancement of QBIC, exciton-polaritons are always accompanied by a large Rabi splitting, which may pave the way for optimizing the performance of polariton devices and realizing low threshold polariton lasing.

In this paper, we design the perovskite nanodisk to support QBIC and realize the strong coupling between QBIC and exciton. We employ the band diagram which is calculated through Finite element method (FEM) to demonstrate the existence of BIC. Then we transform BIC into QBIC by breaking C_2 symmetry of the structure and analyze the connection between QBIC and asymmetry degree. Furthermore, we realize the strong QBIC-exciton coupling and quantitatively study this phenomenon with the aid of the two-coupled oscillators model. We find that the optimized Rabi splitting is maximized to 300.7 meV due to the high Q factor of QBIC. Our scheme provides an original method to explore exciton-polariton at room temperature, which reduces the complexity of the experiments to a great extent. The results have great potential for designing integrated polaritonic devices and pave the way for polariton lasers with ultra-low threshold.

II. STRUCTURE DESIGN

As illustrated in Fig. 1(a), the proposed structure is constituted of perovskite nanodisks with air holes, which are deposited on the silica substrate. The radius and height of each nanodisk are denoted by $R = 150$ nm and $H = 50$ nm respectively, likewise, the radius of air hole labelled by $r = 50$ nm. The unit cell illustrated in the top right inset of Fig. 1(a) is periodical along the x and y direction, with the same periodicity of $P = 350$ nm. It is noteworthy that each air

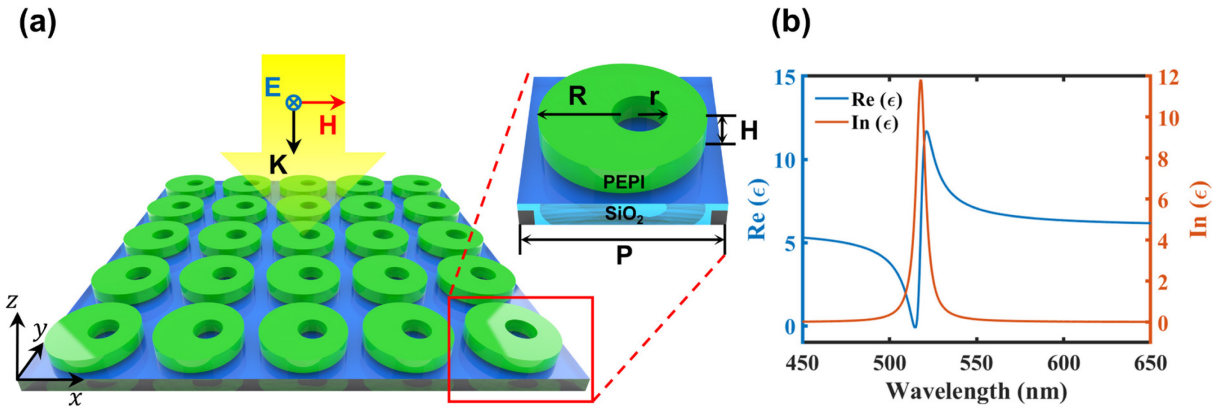

Fig. 1. (a) The metasurface comprised of the PEPI nanodisk under the normally incident plane wave. Inset: the unit cell of PEPI nanodisk with the periodicity of P, radius R and the hight H, as well as a 30 nm off-centerd air hole with the radius r. (b) The real and imaginary components of dielectric function of PEPI.

hole inside the nanodisk has a slight offset of 30 nm along the x-axis to break C_2 symmetry, which leads to the radiation channel opening and hence the ideal BIC collapses into QBIC. The refractive index of the silica substrate is chosen as $n_s = 1.46$ in the visible light wavelength range [5]. The nanodisks are all made out of phenethylammonium lead iodide (PEPI) perovskite with the dielectric function described by the Lorentz oscillator model [5]:

$$\varepsilon(E) = n^2 + \frac{f}{E_{\text{PEPI-exciton}} - E^2 - i\Gamma E} \tag{1}$$

where $n = 2.4$ is the background refraction index, $f = 0.85\ \text{eV}^2$ is the oscillator strength, and exciton energy is determined as $E_{\text{PEPI-exciton}} = 2.394\ \text{eV}$ with the corresponding linewidth of $\Gamma = 0.03\ \text{eV}$. Besides, the real and imaginary parts of Eq. (1) are plotted in Fig. 1(b).

III. Results Discussion and Conclusion

In Fig. 2, we implement the FEM to demonstrate the existence of BIC in the proposed metasurface. Since the metasurface is regarded as passive structure, the oscillator of exciton is determined as : $\varepsilon = n^2$ from Eq. (1), and the effect of the exciton is mainly concentrated in the vicinity of exciton resonance frequency as shown in Fig. 1(b). We suppose that the air hole is situated at the center of the PEPI nanodisk, and utilize eigenfrequency solver to get the corresponding band diagram for the transverse electric (TE) mode in Fig. 2(a). At the high-symmetry point Γ in the first Brillouin zone, we find the symmetry-protected BIC at the wavelength around 504.6 nm, which is encircled by the red line in Fig. 2(a). Additionally, we calculate the corresponding Q factor by taking advantage of the complex frequency of eigenmode and it features an infinite Q factor at the point Γ shown in Fig. 2(b). This convincingly confirms the existence of the BIC, which decouples from the external pump and manifests an exotic phenomenon that the electric field of TE mode is perfectly confined inside the nanodisk as shown in the top right inset in Fig. 2(b).

In order to transform the BIC into QBIC, we make the air hole inside the PEPI nanodisk with an offset along x direction to break C_2 symmetry. We also perform the simulation on the condition of normally incident plane wave and get the transmission map as a function of offset value. As illustrated in Fig. 2(c), the increased offset is accompanied by the variation of transmission dip. To be more specific, when the offset is equal to 0, the dip encircled in Fig. 2(d) vanishes at about 504.6 nm on account of the BIC decoupling from the input light. Along with offset growing from 0 to 80 nm, the C_2 symmetry is broken. BIC collapses into the QBIC which is coupled with the input pump, so the transmission dip arises and turns broader owing to the decrease of Q factor. It is worth mentioning that the wavelength of QBIC manifests a tendency of blueshift with the offset rising, which provides a feasible way to manipulate the QBIC mode.

Above all, in order to facilitate the design of the structure for strong QBIC-exciton coupling, we investigate the optical response of the PEPI metasurface with different periodicity. In Fig. 3(a), we plot the calculated transmission contour map as a function of the period, where the offset of the air hole is 30 nm. It is indicated that the transmission dip of QBIC displays a prominent redshift with the period of the unit cell going up, which inspires us to manipulate the wavelength of QBIC in coincidence with the resonance peak of exciton.

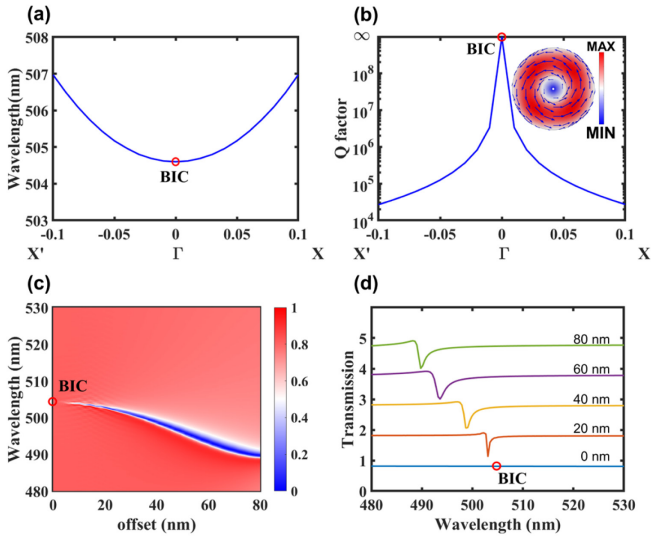

Fig. 2. (a) The band diagram of the metasurface composed of PEPI nanodisk with the air hole centred. Here P = 350 nm , R = 150 nm , r = 50 nm and H = 50 nm . BIC is marked at around 504.6 nm with the red circle. (b) The corresponding Q factor of (a). Inset: the field distribution of BIC TE-like mode at Γ point. (c) The transmission contour map of the metasurface as a function of the air hole offset (0-80 nm). (d) The selected transmission spectrum from (c).

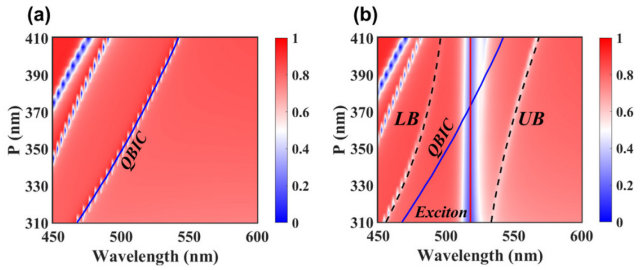

Fig. 3. (a) Simulated transmission map as a function of the period ($P = 310 - 410$ nm) regardless of the exciton oscillator ($f = 0$), where the offset is 30 nm. (b) The transmission map of (a) considering the excitonic oscillator ($f = 0.85$ eV^2). QBIC mode and excitonic mode are marked by the blue line and red line respectively. The UB and LB mode are fitted with the method of the two-coupled oscillators model, marked by black dot lines.

When we take the effect of exciton oscillator into consideration: $f = 0.85$ eV^2, the corresponding transmission map with respect to period is shown Fig. 3(b). As QBIC shifts across resonance wavelength of the exciton, a clear anti-crossing behavior is observed, which is an obvious indication of strong light-matter coupling. Furthermore, we use the two-coupled oscillators model to fit the wavelengths of the lower branch (LB) and upper branch (UB) [12]:

$$\begin{pmatrix} E_{\text{QBIC}} - 0.5i\gamma_{\text{QBIC}} & g \\ g & E_{\text{PEPI-exciton}} - 0.5i\gamma_{\text{PEPI-exciton}} \end{pmatrix} \begin{pmatrix} \alpha \\ \beta \end{pmatrix} = \pm E \begin{pmatrix} \alpha \\ \beta \end{pmatrix} \quad (2)$$

where E_{QBIC} is the energy of QBIC extracted from the transmission, $\gamma_{\text{QBIC}} = 1.8$ meV is the half-width of uncoupled QBIC, and coupling strength is $g = 150.5$ meV . In addition, $E_{\text{PEPI-exciton}} = 2.394$ eV and $\gamma_{\text{PEPI-exciton}} = 0.03$ meV can be obtained from Eq. (1). By solving Eq. (2), we can get the eigenvalue E_- and E_+ corresponding to LB and UB respectively, which is given as:

$$E_{\pm} = (E_{\text{QBIC}} + E_{\text{PEPI-exciton}})/2 - (i\gamma_{\text{QBIC}} + i\gamma_{\text{PEPI-exciton}})/4 \pm \sqrt{g^2 + \left(\delta - 0.5i\left(\gamma_{\text{QBIC}} - \gamma_{\text{PEPI-exciton}}\right)\right)^2 / 4} \quad (3)$$

where the energy difference is $\delta = E_{\text{QBIC}} - E_{\text{PEPI-exciton}}$. Also, we can get the minimum energy difference $\hbar\Omega = \sqrt{4g^2 - (\gamma_{\text{QBIC}} - \gamma_{\text{PEPI-exciton}})^2 / 4}$ between LB and UB, namely Rabi splitting of 300.7 meV, which is enhanced to a high level with the aid of QBIC.

Overall, we have designed the perovskite nanodisk to realize the strong coupling between QBIC and exciton, where the room temperature exciton polaritons have a strong coupling strength of 150.5 meV. We found the BIC at around 504.6 nm according to the band diagram calculated by eigenfrequency solver, and introduced an off-centered air hole into the perovskite nanodisk to make the BIC be coupled with the input plane wave. We also found that the offset of air hole inside the PEPI nanodisk plays a vital role to manipulate the wavelength and linewidth of QBIC, which corresponds to the spectral position and Q factor of QBIC respectively. It has been demonstrated in our work that the wavelength of QBIC can be regulated to be any value by tuning the period of the unit cell. Aiming to achieve the spectral overlap between exciton peak and QBIC, we chose the PEPI nanodisk with a 30 nm off-centered air hole and realized strong exciton-QBIC coupling by tailoring the period. The two-coupled oscillators model has been used to quantitively study this strong coupling between exciton and QBIC. Due to the high Q factor of QBIC, the light matter interaction was enhanced significantly and thus the Rabi splitting was optimized to a high level of 300.7 meV. Our work offers novel guidance to realize the strong coupling between exciton and photon at room temperature, and the BIC-based mechanism in our scheme has high flexibility for tuning Q factor, which facilitates to regulate polaritonic properties including Rabi splitting. Furthermore, due to the strong coherence and nonlinearity of exciton polaritons, the proposed perovskite nanodisk can provide a promising way to realize polariton lasers with low threshold and has great potential for developing ultrafast all-optical circuits and chips.

ACKNOWLEDGMENT

This work was supported by Overseas Research Cooperation Fund of Shenzhen Fundamental Research Program (GXWD20201231165807007-20200827130534001), Youth Science and Technology Innovation Talent of Guangdong Province (2019TQ05X227)

REFERENCES

[1] C. W. Hsu, B. Zhen, A. D. Stone, J. D. Joannopoulos, and M. Soljačić, "Bound states in the continuum," *Nature Reviews Materials*, vol. 1, no. 9, pp. 1–13, 2016.

[2] J. von Neumann and E. Wigner, "Über merkwürdige diskrete Eigenwerte," *Phys. Z*, vol. 30, no. 524, pp. 291–293, 1929.

[3] Y. Plotnik *et al.*, "Experimental observation of optical bound states in the continuum," *Physical review letters*, vol. 107, no. 18, pp. 183901, 2011.

[4] V. Liu, M. Povinelli, and S. Fan, "Resonance-enhanced optical forces between coupled photonic crystal slabs," *Optics express*, vol. 17, no. 24, pp. 21897–21909, 2009.

[5] I. A. Al-Ani, K. As' Ham, L. Huang, A. E. Miroshnichenko, W. Lei, and H. T. Hattori, "Strong coupling of exciton and high-Q mode in all-perovskite metasurfaces," *Advanced Optical Materials*, vol. 10, no. 1, pp. 2101120, 2022.

[6] K. As' ham, I. Al-Ani, W. Lei, H. T. Hattori, L. Huang, and A. Miroshnichenko, "Mie exciton-polariton in a perovskite metasurface," *Physical Review Applied*, vol. 18, no. 1, pp. 014079, 2022.

[7] S. Ghosh *et al.*, "Microcavity exciton polaritons at room temperature," *Photonics Insights*, vol. 1, no. 1, pp. R04, 2022.

[8] J. Kasprzak *et al.*, "Bose–Einstein condensation of exciton polaritons," *Nature*, vol. 443, no. 7110, pp. 409–414, 2006.

[9] H. Deng, G. Weihs, D. Snoke, J. Bloch, and Y. Yamamoto, "Polariton lasing vs. photon lasing in a semiconductor microcavity," *Proceedings of the National Academy of Sciences*, vol. 100, no. 26, pp. 15318–15323, 2003.

[10] A. Amo *et al.*, "Exciton–polariton spin switches," *Nature Photonics*, vol. 4, no. 6, pp. 361–366, 2010.

[11] D. Ballarini *et al.*, "All-optical polariton transistor," *Nature communications*, vol. 4, no. 1, pp. 1778, 2013.

[12] F. Deng, H. Liu, L. Xu, S. Lan, and A. E. Miroshnichenko, "Strong exciton–plasmon coupling in a WS2 monolayer on Au film hybrid structures mediated by liquid Ga nanoparticles," *Laser & Photonics Reviews*, vol. 14, no. 4, pp. 1900420, 2020.